

Electrospinnability of poly(butylene succinate): Effects of solvents and organic salt on the fiber size and morphology

Wattana Klairutsamee,¹ Pitt Supaphol,² Ittipol Jangchud¹

¹Department of Chemistry, Faculty of Science, King Mongkut's Institute of Technology Ladkrabang, Bangkok 10520, Thailand

²Technological Center for Electrospun Fibers and the Petroleum and Petrochemical College, Chulalongkorn University, Bangkok 10330, Thailand

Correspondence to: I. Jangchud (E-mail: kjittipo@kmitl.ac.th or wat_app_chem@hotmail.com)

ABSTRACT: Submicrosized and nanosized fibers of polymers can be formed easily by electrospinning techniques. However, bead formation can occur if inappropriate solvent systems are used. In this study, we focused on investigating the effects of solvents and organic salt on the electrospinnability of poly(butylene succinate) (PBS). Electrospun PBS fibers were obtained from single-solvent systems, that is, systems with chloroform (CF) or dichloromethane, at various concentrations (8–30% w/v). Discrete beads and beaded fibers were still found at every PBS concentration. In this study, the electrospinnability of the PBS solutions in CF were improved by the addition of methanol (MeOH) as a cosolvent and an organic salt [alkyl ammonium ethyl sulfate (AAES)]. The obtained fibers were smooth without any beads, and the diameters were affected by the amount of MeOH and the PBS concentration. The electrospinnability of PBS could be enhanced by the addition of a cosolvent with a high dielectric constant or organic salt (AAES). Moreover, the diameters of the electrospun PBS fibers decreased with increasing AAES concentration. We found that the presence of MeOH (30 vol %) and the addition of AAES caused an increase in the crystallinity of the PBS fibers. Therefore, we concluded that bead-free ultrafine PBS fibers could be obtained through the addition of the cosolvent and the organic salt. © 2015 Wiley Periodicals, Inc. *J. Appl. Polym. Sci.* 2015, 132, 42716.

KEYWORDS: biodegradable; electrospinning; fibers; morphology; nanostructured polymers

Received 26 January 2015; accepted 12 July 2015

DOI: 10.1002/app.42716

INTRODUCTION

Electrospinning has been proven to be useful for producing ultrafine fibers with average diameters in range of micrometers to nanometers. The advantages of electrospun fibers include a high specific-surface-area-to-volume ratio and nonwoven mats with small pore sizes.^{1–3} These characteristics are essential for various applications, including those in nanocatalysis, tissue engineering scaffolds, protective clothing, biomedicine, pharmaceuticals, optical electronics, healthcare, biotechnology, defense and security, and environmental engineering.^{3–7} The morphology of the electrospun fibers plays a crucial role in the physical and mechanical properties of the final products to be used in certain applications. Therefore, the electrospinning of uniform fibers without bead defects is essential. Parameter effects on the morphology and arrangement of the electrospun fibers can be divided into three categories: solution properties (polymer concentration, solvent volatility, surface tension, and solution conductivity), process parameters (applied voltage, polymer flow rate, and capillary–collector distance), and ambient parameters.^{8–10} The effects of these parameters on the morphology,

fiber diameter, and bead formation of the electrospun fibers have been investigated.^{11–17} The solvent is one of the main contributors toward the solution properties (e.g., conductivity, surface tension, boiling point). The dielectric constant (ϵ) is practically a measure of the electron-holding capacity. Solvents with high ϵ s added to the electrospinning of a solution can interact differently with the electrostatic field.^{11,12,17} Wannatong *et al.*¹² reported correlations between the properties of the solvent on the productivity and morphological appearance of electrospun polystyrene fibers. The productivity of the as-spun PS fibers increased with increasing dielectric constant and dipole moment of the solvents. The results suggest that there were strong correlations between the solvent properties and the morphological appearance of the as-spun fibers and the productivity of the process. Moreover, additives, that is, salts and surfactants, have been proven to be useful in improving the electrospinnability and in controlling the fiber morphology through the modification of the solution properties, including the conductivity, viscosity, and surface tension.^{18–21} Inorganic salts (LiCl, NaNO₃, NaCl, and CaCl₂), cationic surfactants,¹⁹ hyperbranched

Table I. Properties of the Solvents Used in This Study^{35,36}

Solvent	Boiling point (°C)	Dipole moment (Debye)	ϵ	Surface tension (mN/m ²)	Viscosity (mPa s)	Hansen solubility parameter (MPa) ^{1/2}
CF	61.2	1.01	4.8	26.6	0.54	19.0
DCM	39.8	1.60	8.9	27.2	0.79	19.8
DMF	153.0	3.82	37.0	36.3	0.79	24.0
MeOH	64.7	1.60	32.6	22.1	0.54	29.6

Hansen solubility parameter of PBS = 20.3 (MPa)^{1/2}.^{37,38}

poly(ester amine),²⁰ organic salts,²¹ and ionic liquids²² are used to add to polymer solutions to improve the electrospinnability of polymer solutions through increases in the conductivity of the solution.

Moreover, the effects of the process parameters also influence the morphology and diameter of electrospun fibers. The optimal conditions vary in different polymer–solvent systems. Bead defects in electrospun fibers may be found from inappropriate field strengths.^{3,12,23,24} Patra *et al.*²⁴ designed experiments to establish a desirable set of conditions for producing electrospun PLLA nanofibers. They found that a low polymer concentration (4% w/v) and high applied voltage (10 kV) appeared to be the best choice for obtaining the finest diameter. The flow rate of polymer solutions can influence the jet velocity and material transfer rate. A lower feed rate is more desirable so the solvent has enough time to evaporate.^{23,25} There should always be a minimum flow rate in the spinning solution. High flow rates can cause beaded fibers because of the unavailability of a proper drying time before the collector is reached.^{12,25} The distance between the needle and collector is also one of the key factors in controlling the fiber diameter and morphology. An optimal distance is required to give an optimal field strength and sufficient time to dry before the fibers reach the collector. Suboptimal distances are either too close or too far, and beads have been observed with the electrospinning of PVA²⁶ and gelatin.²⁷ It has been reported that flatter fibers can be produced at closer distances, but with increases in the distance, rounder fibers have been observed.

Poly(butylene succinate) (PBS) and its copolymers are commercially available aliphatic polyesters with interesting properties, including biodegradability, melt processability, and good mechanical and thermal properties. Because of their excellent mechanical properties and processability, they can be applied to a number of applications, such as packaging films, bags, flushable hygiene products, mulch films biomedical materials, and nonwoven electrospun PBS fibers. PBS is a biodegradable synthetic polymer with good biocompatibility compared to poly(lactic acid) or poly(glycolic acid).²⁸ Because of their great properties, electrospun PBS fibers can be extended further to medical treatments, textiles, biomedical applications, and more. The electrospinning of PBS solutions has been widely studied.^{29–34} In the electrospinning of the polymer solution, PBS is able to be dissolved in various solvents, such as dichloromethane (DCM), chloroform (CF), HFIP, and *o*-chlorobenzene. However, bead-free uniform electrospun PBS fibers have been reported when various added solvent sys-

tems were tested.^{29–34} Jeong *et al.*³³ reported that ultrafine PBS fibers were successfully prepared by the electrospinning of a PBS solution in several mixed-solvent systems, including CF/CE, DCM/CE, and CF/3-CP. Moreover, PBS fibers were prepared by the electrospinning of a 13 wt % PBS solution in 7 : 3 CF/CE and annealed *in vacuo* at 95°C for 4 days. These fibers had a very high crystallinity compared to those of ultrafine fibers of common polymers.³³ Tserki *et al.*³⁴ studied the morphology and thermal properties of PBS fibrous mats electrospun from mixed-solvent systems. Microbeads, beads in threads, and ultrafine fibers were observed from the electrospinning of PBS solutions in DCM/*N,N*-dimethylformamide (DMF) mixtures; these depended on the ratios of the two solvents. Moreover, they also reported wide-angle X-ray diffraction and differential scanning calorimetry (DSC) analysis showing a reduction in the crystallinity. Although electrospun PBS bead-free fibers have been reported when various solvent systems were investigated,^{31–34} no report has been conducted to illustrate the effects of organic salts and solvents with high dielectric constant on the PBS solution properties and the morphology of PBS fibers. In this study, we focused on studying the effects of the addition of an organic salt [alkyl ammonium ethyl sulfate (AAES)] on the solution properties, morphological appearance, and diameters of electrospun PBS fibers; we also studied the effect of dielectric constant of the solvent systems and the solution concentrations. The single-solvent systems investigated in this study were CF and DCM. The mixed-solvent systems were CF–DMF and CF–methanol (MeOH). Changes in the fiber diameter and morphology of the electrospun PBS fibers were investigated in terms of the solution viscosity, surface tension, dielectric constant and conductivity. Moreover, the effects of the solution properties on the thermal properties of the electrospun PBS fibers were also studied.

EXPERIMENTAL

Materials

Commercial PBS (Bionolle 3001, number-average molecular weight = 190 kg/mol, glass-transition temperature = –42°C, melting temperature = 92°C) was purchased from Showa High-polymers Co., Ltd. PBS was dried *in vacuo* at 50°C for 36 h before use. The solvents used in this study were CF from BDH (United Kingdom); DCM, MeOH, and DMF from Aldrich (Germany); and AAES Effka 6782 from BASF Co., Ltd. These chemicals were analytical grade and were used without further purification. Some of the properties of these solvents are summarized in Table I.

Table II. Ratios of Mixed-Solvent Systems at 12% w/v PBS Concentrations

Mixed-solvent systems	Ratios of solvents (v/v)
CF-DMF	50 : 50, 70 : 30, and 90 : 10
CF-MeOH	

Preparation and Characterization of the PBS Solutions

PBS solutions were prepared in either a single solvent and in mixed-solvent systems at room temperature. In the single-solvent systems, five concentrations, that is, 8–30% w/v were prepared in the CF and DCM solvents. In mixed-solvent systems, PBS was dissolved in CF-DMF and CF-MeOH. The ratios of mixed solvents used in this study are shown in Table II. The PBS concentration in the mixed-solvent systems was fixed at 12% w/v. All of the PBS solutions were stirred at room temperature for 2 h with a magnetic stirrer. The solution properties, that is, the viscosity, surface tension, and conductivity, were measured for all solutions with a Brookfield TVB-10 programmable viscometer, CSC Scientific tensiometer, and Jeneway 4130 conductivity meter, respectively.

Preparation of PBS Solutions with Organic Salts

To study the effects of the organic salt (AAES) on the electrospinnability, solutions of 12% w/v PBS in CF were prepared with the addition of different salt concentrations, that is, 0.25, 0.5, and 1% w/v. These solutions were stirred at room temperature for 5 min. Afterward, a 12% w/v PBS solution was stirred with a magnetic stirrer for 2 h before the solution properties (i.e., viscosity, conductivity, surface tension) were measured.

Electrospinning Process Setup

The electrospinning setup used in this study consisted of a 50-mL glass syringe, a stainless needle with a flat tip

Table III. Viscosity, Conductivity, and Surface Tension of the As-Prepared PBS Solutions in CF and DCM

Solvent	PBS concentration (% w/v)	Viscosity (mPa s)	Conductivity ($\mu\text{S}/\text{cm}$)	Surface tension (mN/m^2)
CF	8	94.3	0.03	34.0
	12	115	0.04	34.2
	16	158	0.05	34.5
	20	191	0.04	35.2
	30	281	0.03	35.4
DCM	8	96.0	0.15	34.5
	12	118	0.14	35.2
	16	160	0.15	35.5
	20	195	0.15	35.4
	30	285	0.14	35.6

(i.d. = 0.91 mm) used as a spinneret, a Γ high-voltage D-ES30PN/M692 direct-current power supply (20 kV, Florida), and an aluminum sheet on a rotating drum as a screen collector. The distance between the nozzle tip and the outer surface of the collector was fixed at 18 cm. The emitted electrode of positive polarity was attached to the needle and ground-attached on the rotating drum at a fixed speed of 95 rpm. Both the needle and the syringe were tilted about 45° from a horizontal baseline to maintain the constant presence of a droplet at the tip of the needle. The collection time was fixed at 1 h.

Morphological Study

The morphological appearance of the electrospun PBS fibers was observed with a JEOL JSM-6400 scanning electron microscope. We prepared specimens for scanning electron microscopy (SEM) observation by cutting an Al sheet covered with the as-

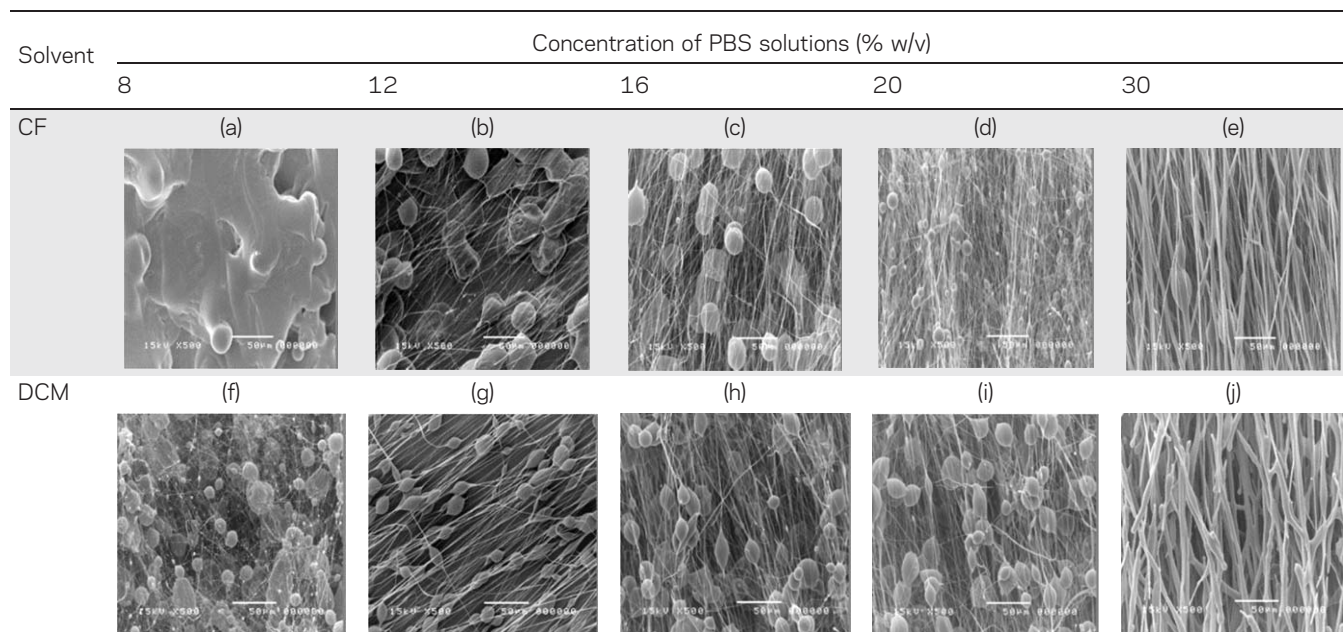
Table IV. SEM Images (500 \times) of the Electrospun PBS Obtained from 8, 12, 16, 20, and 30% w/v PBS Solutions in Single-Solvent Systems

Table V. Viscosity, Conductivity, and Surface Tension of the As-Prepared PBS Solutions in the Mixed-Solvent Systems as a Function of the Ratio of the Solvents

Solvent system	Ratio of the mixed solvents (v/v)	Viscosity (mPa s)	Conductivity ($\mu\text{S}/\text{cm}$)	Surface tension (mN/m^2)
CF	100	115	0.04	34.2
CF-DMF	90 : 10	120	2.00	37.9
CF-MeOH	70 : 30	118	2.80	33.1
	90 : 10	113	1.90	34.0

spun materials and carefully affixed to copper stubs. Each specimen was gold-coated with a JEOL JFC-1100E sputtering device before observation under SEM. The diameters of the electrospun fibers or beaded fibers were measured directly from

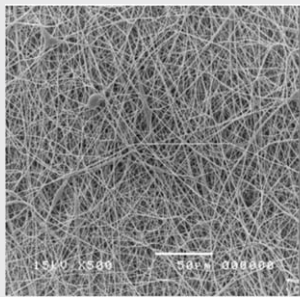
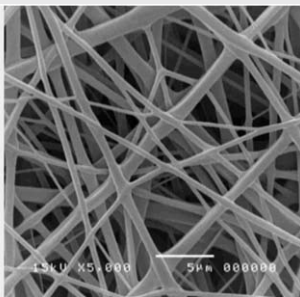
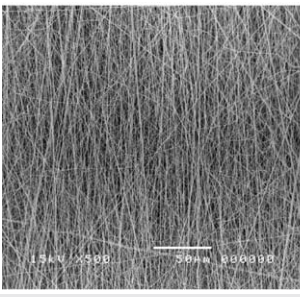
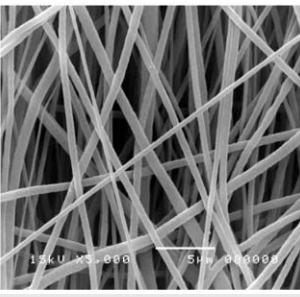
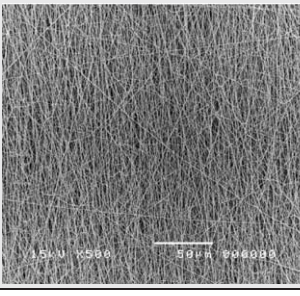
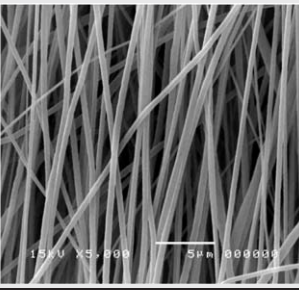
selected SEM images with SemAphore 4.0 software. The reported diameter values for each of the samples were averaged from at least 50 measurements. For the beaded fibers, the fiber diameters were measured between beads.

RESULTS AND DISCUSSION

Single-Solvent Systems

In this part, CF and DCM were chosen as single solvents for preparing PBS solutions. The effects of the PBS concentrations on the PBS solutions and the morphologies of the electrospun fibers were also investigated. CF and DCM were able to dissolve PBS pellets to form a clear solution within 2 h. Table III summarizes the viscosity, conductivity, and surface tension of the as-prepared PBS solutions. As expected, the viscosities of the PBS solutions in both solvents increased with increasing PBS concentration. Insignificant changes were observed in the conductivity and surface tension of the PBS solutions. Table IV

Table VI. SEM Images of Electrospun Fibers and Diameters of Electrospun PBS Fibers Produced from a 12% w/v PBS solution in a Variety of Mixed-Solvent Systems: 90 : 10 v/v CF-DMF and 90 : 10 and 70 : 30 v/v CF-MeOH

Solvent system	Ratio of mixed solvents (v/v)	Magnification		Average fiber diameter (nm)
		500 \times	5000 \times	
CF-DMF	90 : 10			743 \pm 55
CF-MeOH	90 : 10			575 \pm 84
	70 : 30			480 \pm 70

These fibers were electrospun under an applied electrostatic field strength of 20 kV/18 cm.

Table VII. Viscosity, Conductivity, and Surface Tension of the Solutions and Characteristic of the Electrospun Fibers Obtained from 8, 12, 16, and 20% w/v PBS Solutions in the Mixed Solvent 70 : 30 v/v CF–MeOH

Concentration % w/v	Shear viscosity (mPa s)	Surface tension (mN/m)	Conductivity ($\mu\text{S/cm}$)
8	98	32.8	2.83
12	118	33.1	2.81
16	184	33.4	2.83
20	202	33.3	2.85

shows SEM images of the electrospun fibers obtained from the PBS solution in the single-solvent systems at various concentrations. As shown in Table IV, sprayed droplets obtained from the electrospinning process were found when we used a PBS concentration of less than 12% w/v. At this low concentration (8% w/v), this effect was attributed to the poor chain entanglement density in the PBS solution. It had insufficient resistance to the electrical field, and this resulted in polymer jet breakup to the PBS droplets. When the PBS solution concentration was increased (12–30% w/v), the morphology changed into beaded fibers. Moreover, the bead sizes of the electrospun PBS fibers had a tendency to decrease as the PBS concentration increased. Although CF was able to dissolve PBS pellets to form a clear solution as a result of the PBS fibers being electrospun from PBS solutions in CF, small beaded fibers were still present at all concentrations. This result was also reported by Tian³⁵ because the PBS–CF solution was unsuccessfully electrospun because of large beaded fibers. In theory, the electrospinning mechanism is governed under two instabilities: that is, axisymmetric varicose instability (Rayleigh instability) and nonaxisymmetric whipping instability.^{38,39} These instabilities are determined by factors related to the solution properties and operating conditions, including the solution viscosity, conductivity, surface tension, and strength of the applied electrostatic field.^{38,39} Two instabilities can be clearly explained with six forces.^{17,40}

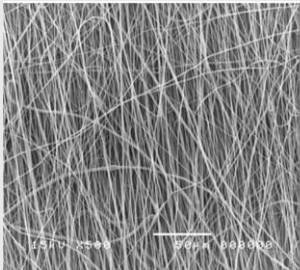
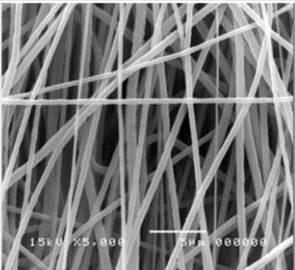
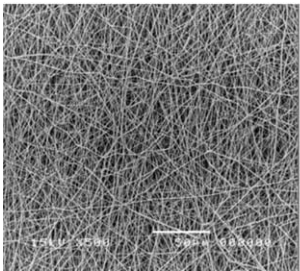
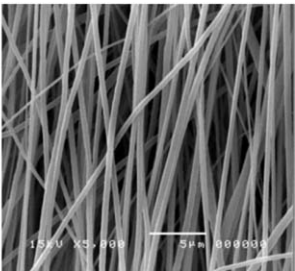
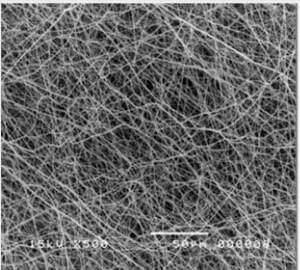
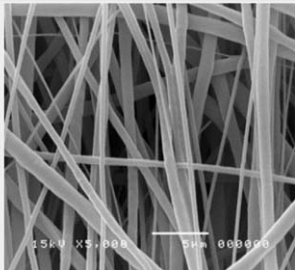
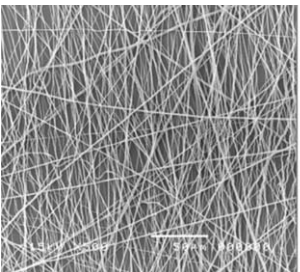
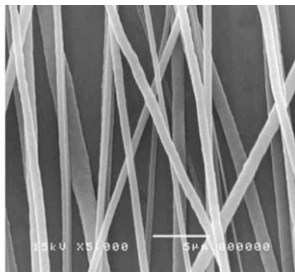
1. The gravitation force toward the collector plate in vertically arranged apparatus. This force depends on the density of the polymer solution.
2. The electrostatic force, which is used to extend the jet polymer and propel it toward the grounded collector. This force is determined by the applied electric field.
3. The coulombic force, which occurs on the surface of the polymer jet. The magnitude of this force is dependent on the characteristic of the polymer and solvent. It is responsible for the thinning or stretching of the charged jet during its flight to the target. This force is related to the charged density of the polymer and the conductivity of the polymer solution.
4. The viscoelastic force, which works against the elongation of the jet in the electric field. This force depends on the polymer molecular weight, solvent, and type of polymer.
5. The surface tension force, which works against the stretching of the surface of the charge jet.

6. The friction, or drag force, which acts between the surface of the polymer jet and the surrounding air.

Among these forces, only the coulombic, viscoelastic, and surface tension forces dominate the formation of beads and the thinning of the charged jet during its flight to the grounded target. Axisymmetric varicose instability (Rayleigh instability) results from the surface tension of the solution^{1,2} and produces drops rather than fibers. It can occur when the strength of the electrical field is lower or the viscosity of the solution is below the critical value. Nonaxisymmetric instability (whipping instability) is presented by the electrostatic field and charge density of the polymer jet. It results in the bending and stretching of the jet through a rapidly spiraling motion. The polymer solution factors, that is, the viscosity of the polymer solution and the conductivity of the solution, can be used to suppress the Rayleigh instability. The solution viscosity is dominated by the solution concentration or the molecular weight. This factor is related to the extent of polymer chain entanglement. The latter is governed by the conductivity of the polymer solution. In this study, uniform PBS fibers could not be obtained from the single-solvent system, even though the PBS concentrations were increased up to 30% w/v. This reason was considered to have derived from the low conductivity of CF ($\epsilon = 4.8$), as shown in Table I. Then, the low conductivity of the PBS solution in CF was unable to suppress the Rayleigh instability. It promoted beaded fibers rather than uniform fibers.

In the case of the PBS solution in DCM, the morphology of the electrospun fibers obtained from all of the concentrations were significantly different compared with the PBS fibers obtained from solutions in CF. The beaded fibers obtained from the PBS solution in DCM was found at 8% w/v (image f in Table IV) rather than sprayed droplets (image a in Table IV). This might have derived from the conductivity of the PBS solution in DCM, which was higher than that of the PBS solution in CF because the ϵ value of DCM ($\epsilon = 8.9$) was higher than that of CF ($\epsilon = 4.8$). The effects of the solvent ϵ on the fiber morphology have been reported by several research groups.^{12,17,40,41} Although the solution concentration is one of key factors that can suppress the Rayleigh instability, in this study, the suppressed effect was dominated at high concentrations of PBS in DCM. It resulted in discontinuous fibers at 30% w/v, as shown in the inserted image j in Table IV. Although DCM could dissolve PBS to form a clear solution, the resulting PBS solutions were difficult to use in electrospinning processes because the solutions often clogged the tip of nozzle. Clogging by the solution was due to the low boiling point of the DCM (39.8°C); this resulted in a rapid evaporation of the solvent. At this point, nonuniform PBS fibers were still observed at high concentrations because of the low conductivities of the PBS solution in both single solvents (Table III) because CF and DCM had low dielectric constant, as shown in Table I. Therefore, attempts to increase the solution conductivity were carried out in this study by the addition of another solvent with a high dielectric constant as mixed-solvent systems or by the addition of an organic salt (AAES) to improve the electrospinnability of the PBS solutions.

Table VIII. SEM Images of the Electrospun PBS Fibers and Diameter of Electrospun PBS Fibers Produced from 8, 12, 16, and 20% w/v PBS in the Mixed Solvent 70 : 30 v/v CF–MeOH

Concentration (% w/v)	Magnification		Average fiber diameter (nm)
	500×	5000×	
8	8(a)		404 ± 55
			
12	8(b)		480 ± 70
			
16	8(c)		664 ± 50
			
20	8(d)		874 ± 86
			

Mixed-Solvent Systems

The effects of the ϵ values of the solvents on the morphology of the electrospun PBS fibers were studied. To investigate the effects of ϵ of the solvent on the morphology of the electrospun PBS fiber, solvents with high ϵ s, that is, DMF and MeOH, were chosen to improve the electrospun fibers to eliminate bead defects. In this part, the PBS concentration in the mixed-solvent systems was fixed at 12% w/v. The applied electrostatic field strength was also fixed at 20 kV/18 cm.

CF–DMF. DMF is one of the solvents with high boiling point and dielectric constant values.⁴¹ Lee *et al.*¹³ reported that smooth nanofibers of PCL could be electrospun by the addition of DMF to a PCL solution in DCM. DMF decreased the viscosity and increased the electrical conductivity of the PCL solution. In this study, DMF was used to increase the conductivity of the PBS solution in CF. Solubility tests of PBS in the mixed-solvent system were first performed at different various mixing ratios of CF to DMF. We found that PBS could not be dissolved in CF–

Table IX. Viscosity, Conductivity, and Surface Tension of Solutions Obtained from a 12% w/v PBS Solution in CF with Different Loadings of AAES Ranging from 0 to 1% w/v

Concentration of salts (% w/v)	Shear viscosity (mPa s)	Surface tension (mN/m)	Conductivity (μ S/cm)
0	115	34.2	0.03
0.25	114.7	33.8	1.4
0.5	114.5	33.2	5.0
1	114	33.0	17.8

DMF within 2 h when the DMF loading was higher than 10% v/v. Therefore, this ratio was chosen to study in this work. The effects of DMF addition on the PBS solution properties and morphology of the electrospun PBS are shown in Tables V and VI, respectively. As expected, the conductivity of the PBS solution in CF increased after the addition of DMF to the PBS solution. The viscosity and surface tension of the PBS solution increased slightly compared with those of the PBS solutions in pure CF. The morphologies and average fiber diameters of the PBS fibers prepared with those of the 12% w/v PBS solution in the mixed-solvent system are shown in Table VI (image 6a). The addition of DMF into the electrospinning PBS solution was shown to improve the PBS fiber morphology (as shown in image 6a in Table VI). The electrospinnability of the resulting PBS solution in this mixed-solvent system was improved due to the dielectric constant of DMF. The increased conductivity of the PBS solution in mixed solvent led to an increase in the surface jet charges. Under a given electric field, the increased conductivity resulted in stronger elongational forces imposed on the jet. This caused self-repulsion of the excess charges on the surface. This effect suppressed the Rayleigh instability and yielded enhanced whipping action and minimized defects. However, few beaded and large PBS fibers were found in this solvent system. This was attributed to the high boiling point of DMF.

CF–MeOH. From the solvent properties shown in Table I, MeOH is one of the solvents with a high dielectric constant. We found that PBS could not be dissolved in CF–MeOH within 2 h when the MeOH loading was higher than 30% v/v. A 12% w/v PBS solution in these mixed-solvent systems was studied in this part. Some properties, that is, the viscosity, surface tension, and conductivity of the PBS solution are summarized in Table V. As expected, the conductivity of the PBS solution increased with the addition of MeOH into the mixed-solvent system as compared to the PBS solution in CF. This could be explained by the fact that the dipole moment and dielectric constant of MeOH were higher than those of CF. This resulted in an increase in the ion species in the mixed solvent. Table VI shows that the amount of MeOH added to the PBS solution had significant effects on the structures of the electrospun PBS fibers. As the MeOH loading was increased from 0 to 30%, the morphologies of the electrospun PBS fibers were changed from beaded fibers to smooth fibers. Moreover, the average diameters of the PBS fibers decreased from 575 nm (image 6b, Table VI) to 480 nm (image 6c, Table VI) with increasing MeOH content, as shown

in Table VI. This was likely a result of the increased dielectric constant of MeOH (ϵ of MeOH = 32.6 and ϵ of CF = 4.8). The results are similar to those of Lee *et al.*,¹³ Nitanan *et al.*,¹⁰ and Wannatong *et al.*¹² With the addition of high- ϵ solvent into the polymer solution, this led to increased conductivity in the solution. The surface charges of the spinning jet obtained from electrospinning were increased. This caused the coulombic stretching forces to increase and resulted in stronger elongation forces imposed on the jet; this was caused by the self-repulsion of the excess charges on the surface. The increasing charge density was able to promote the whipping or bending instability because the high surface charges simultaneously suppressed the axisymmetric modes and promoted fluid bending under a governed electric applied field. These phenomena might have resulted in a higher degree of elongation of the jet. This process occurred during the transit of the solution jet to the collector. Smooth defect-free ultrafine PBS fibers with smaller diameters were obtained with these systems. From previous results, it was clear that continuous ultrafine fibers were obtained dramatically; this depended on the types of solvents and optimal ratios of mixed-solvent system.

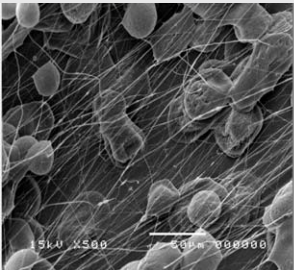
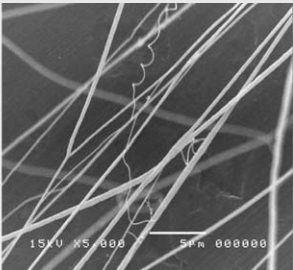
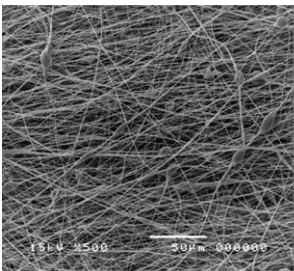
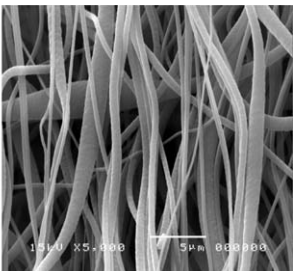
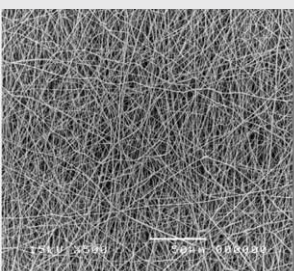
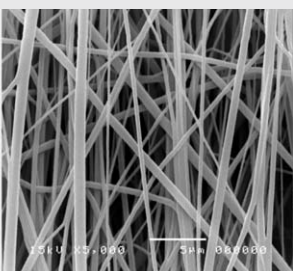
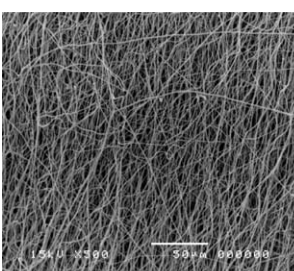
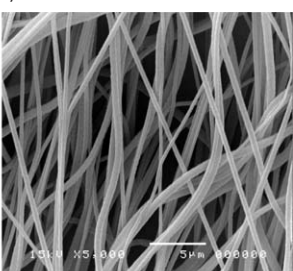
Effects of the PBS Concentrations in CF–MeOH

Previously, 70 : 30 v/v was the best ratio of CF–MeOH for preparing ultrafine fibers without bead defects from the electrospinning process. In this part, to investigate the effects of the solution concentrations on the morphology and size of the electrospun PBS fibers, PBS solutions of different concentrations (8, 12, 16, and 20% w/v) were prepared. The solution properties, that is, the viscosity, surface tension, and conductivity, are presented in Table VII. As expected, the viscosities of the solutions largely increased with increasing solution concentration, whereas the conductivities and surface tensions of the PBS solutions increased slightly. Table VIII shows the SEM images of the fibers and average diameters. At 8% w/v PBS solution (image 8a), a few beaded fibers were obtained. This low concentration resulted in a low viscoelastic force because the chain entanglement in a given solution was appreciably less than a critical value. This might not have been enough to form a stable polymer jet. Therefore, it was not sufficient to counter the stretching forces from both the electrostatic and coulombic repulsion forces. The overstretching of the charged jet, as a result of these forces, resulted in a partial breakup of the jet. The surface tension of the solution tended to minimize the surface areas by forming individual droplets. Beaded fibers, therefore, were formed on some of the fibers^{42–45} with this PBS concentration. However, continuous and smooth fibers were obtained by the spinning of 12–20% w/v (images 8b–8d) PBS solutions. At these high concentrations, the high viscoelastic force was enough against the electrostatic stretching force. These high PBS concentrations resulted in more chain entanglement and yielded an increase in the viscosity of the polymer solution. The Rayleigh instability was suppressed when these concentrations were used.

Effects of the Organic Salt (AAES)

As mentioned previously, salts have been proven to be useful in improving the electrospinnability and controlling the fiber morphology through the modification of the solution properties, that is, the conductivity, viscosity, and surface tension of the

Table X. SEM Images of the Electrospun PBS Fibers and Diameters of the Electrospun PBS Fibers Obtained from 12% w/v PBS in CF with Various Concentrations of AAES

Concentration (% w/v)	Magnification		Fiber diameter (nm)
	500×	5000×	
0	10(a)		348 ± 44
			
0.25	10(b)		503 ± 55
			
0.5	10(c)		381 ± 28
			
1	10(d)		373 ± 28
			

Electrospun PBS fibers from solution in pure CF were only measured on the fiber sections between the beads.

solution. In this part, AAES was chosen as the salt for increasing the PBS conductivity because it consisted of organic cations and inorganic anions. Table IX shows the PBS solution properties, that is, the viscosity, surface tension, and conductivity, before and after the addition of AAES (0.25–1% w/v). It was clear that the addition of AAES to the PBS solution caused a significant increase in the conductivity of the PBS solution. However, the viscosity and surface tension of the PBS solutions

in CF decreased slightly when AAES was added. Table X shows the SEM images of the ultrafine PBS fibers and average fiber diameters electrospun from 12% w/v PBS solution with different concentrations of AAES. Small beaded fibers were still found when 0.25% w/v (image 10a, Table X) AAES was added. As shown in Table X, the addition of salt also increased the charge density in the ejected jet. This yielded a stronger elongation force of the polymer jet because of the self-repulsion of the

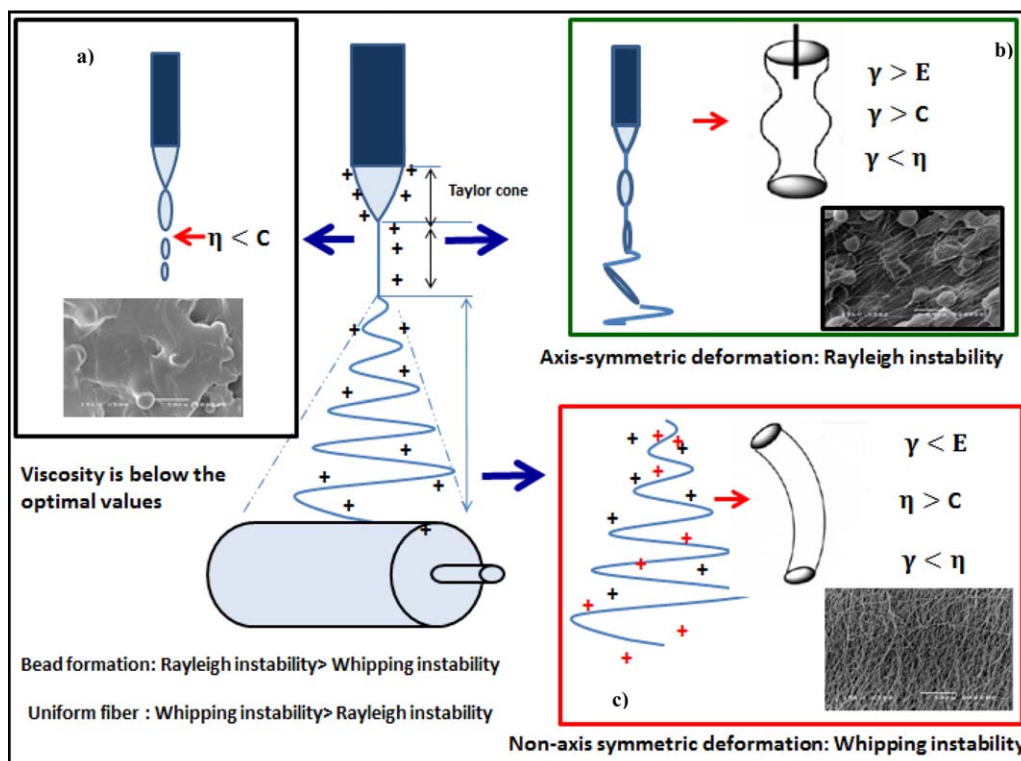


Figure 1. Possibility mechanism of electrospun fibers proposed with the interaction of various forces caused by the viscosity (η), electrostatic force (E), surface tension (γ), and coulombic stretching force (C): (a) formation of a droplet defect from the electrospinning process, (b) beaded fiber from axis-symmetric varicose instability (Rayleigh instability), and (c) nonaxisymmetric whipping instability.^{17,38–40} [Color figure can be viewed in the online issue, which is available at www.interscience.wiley.com.]

excess charges under the electrical field; this resulted in a substantially straighter shape and a smaller diameter in the electrospun fibers. This suppressed the Rayleigh instability, enhanced the whipping instability, and reduced defects. A uniform fiber morphology with a narrow diameter distribution was obtained because the charged density of polymer jet was increased with the addition of the organic salt (AAES). The average diameters

of electrospun fibers obtained from the solution with AAES decreased with increasing AAES concentration, as shown in Table X (image 10b–10d).

Possible mechanisms used for the fabrication of ultrafine electrospun polymer fibers are summarized in Figure 1 to obtain a better understanding of the effects of balanced forces during the electrospinning process. The viscoelastic, coulombic, electrostatic forces, and surface tension are the most important forces that influence fiber formation. Two instabilities of the polymer jet related to these forces are involved in this mechanism. These forces can be adjusted in balanced conditions to prevent bead formation. Increased charge density of the polymer jet through the addition of high dielectric constant solvents or organic salt affected the fiber diameters and morphologies of the electrospun fibers. In this study, sprayed droplets of PBS were obtained from the electrospinning of PBS solutions in both single solvents. This behavior could be explained by Figure 1(a). A very low viscosity of the PBS solutions resulted in low chain entanglement densities in the polymer jet. This was not sufficient to counter the stretching forces from both electrostatic and coulombic repulsion forces. Eventually, this caused the jet to break up and led to droplets. These defects could be suppressed by increases in the charge density of the polymer jet or solution viscosity. The effects of the charge density of the polymer jet and solution viscosity on the morphology of the polymer fibers is explained in Figure 1(b). Through increases in the viscosity of the PBS solution, the chain entanglement density of polymer

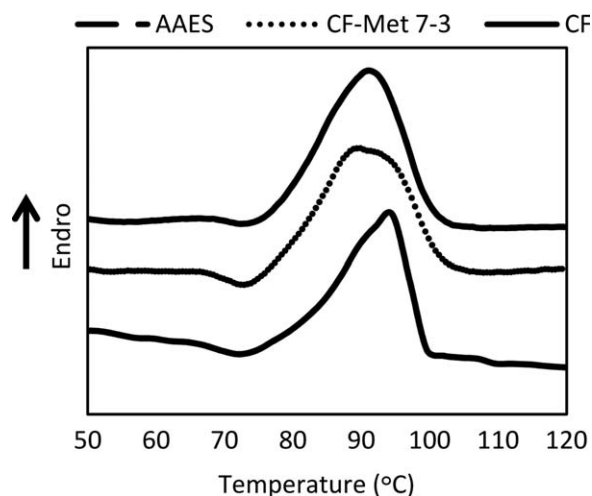


Figure 2. DSC thermograms of the electrospun ultrafine PBS fibers from solution in CF with and without 1% w/v AAES and the mixed-solvent system 70 : 30 v/v CF–MeOH.

Table XI. Thermal Properties of the Ultrafine PBS Fibers Obtained from an Electrospun PBS Solution 12% w/v in CF with Various Salt Concentrations

Solvent	Salt concentration (% w/v)	Melting temperature (°C)	Melting enthalpy (J/g)	Crystallinity (%)
100 v/v CF	0	94.4	38.7	19.4
	0.25	96.3	48.2	24.1
	0.50	98.5	48.5	24.3
	1.00	96.3	56.2	28.1
70 : 30 v/v CF-MeOH	0	92.8	46.8	23.4

Heat of fusion for PBS = 200 J/g.³³

molecules increased. This suppressed the breakup of the polymer jet. However, the low conductivity of the PBS solutions led to very low charge densities of the PBS jet. Therefore, it could not suppress the Rayleigh instability. The positive ions shown in Figure 1(c), that is, the black positive ion obtained from the strong electrostatic field and the red positive ion obtained from the increase in the polymer solution conductivity, enhanced the charge density of the polymer jet and led to a suppressed Rayleigh instability. This promoted beaded fibers rather than uniform fibers. Figure 1(c) explains the results of the enhancement in the charge density of the polymer jet through increases in the conductivities of the PBS solutions. In this study, high dielectric constant solvents and an organic salt (AAES) were added to the PBS solution to increase the charge density of the polymer jet. The great excess density of the polymer jet resulted in stronger elongation forces; this was caused by self-repulsion of the excess charges on the surface. The Rayleigh instability could be suppressed, whereas the bending and whipping instabilities were enhanced; this yielded a defect reduction. Finally, a uniform fiber morphology with a narrow size distribution was obtained. Therefore, it was clear that the Rayleigh instability is one of the most important factors that cause bead formation.

Thermal Properties

Figure 2 and Table XI show the DSC thermograms and thermal properties of electrospun PBS fibers obtained from 12% w/v PBS solutions with and without AAES. We found that additions of both AAES salt and MeOH cosolvent enhanced the percentage crystallinity of the PBS fibers compared to that of PBS fibers spun from a single-solvent (CF) solution. This suggested that the conductivity of the polymer solutions influenced the chain orientation and crystallization of the PBS chains. The increased conductivity of the PBS solution resulted in a high degree of elongation of the jet. This increased the alignment of the molecular chains along the fiber axis. Moreover, the degree of crystallinity of the PBS fiber increased as the amount of AAES increased from 0 to 1% w/v, as shown in Table XI.

CONCLUSIONS

In this study, the effects of the solvent systems, solution concentrations, and organic salt (AAES) addition on the electrospinnability of PBS and fiber morphology were investigated. In the case of the single-solvent systems (CF and DCM), bead formation was still present at all concentrations because of the low

solution conductivities. We found that the bead problems could be solved by the addition of DMF or MeOH cosolvents and the AAES organic salt. The cosolvents and salt had significant effects on the solution conductivity and PBS fiber morphology. It was clear that continuous ultrafine fibers could be obtained; this greatly depended on the types of solvents and optimal ratios of the mixed-solvent systems. The addition of AAES to the PBS solution resulted in a dramatic increase in the solution conductivity. The fiber diameters decreased when the AAES loading was increased. Moreover, the additions of the AAES salt and MeOH cosolvent enhance the percentage crystallinity of PBS. We found that the conductivity of the PBS solution was one of the most important factors affecting the morphology, fiber diameter, and thermal properties of the electrospun PBS fibers.

ACKNOWLEDGMENTS

The authors acknowledge support from Chulalongkorn University (through invention and research grants from the Ratchadapesek Somphot Endowment Fund), the Petroleum and Petrochemical Technology Consortium (through a Thai governmental loan from Asian Development Bank), and the Petroleum and Petrochemical College, Chulalongkorn University.

REFERENCES

- Huang, A. Z.; Zhang, Y. Z.; Kotaki, M.; Ramakrishna, S. *Compos. Sci. Technol.* **2003**, *63*, 2223.
- Greiner, A.; Wendroff, J. H. *Angew. Chem. Int. Ed.* **2007**, *46*, 5670.
- Ramakrishna, S.; Fujihara, K.; Teo, W. E.; Yong, T.; Ma, Z.; Ramaseshan, R. *Mater. Today* **2006**, *9*, 40.
- Yoo, H. S.; Kim, T. G.; Park, T. G. *Adv. Drug Delivery Rev.* **2009**, *61*, 1033.
- Wu, Y.; He, J. H.; Xu, L.; Yu, J. Y. *Int. J. Electrospun Nanofibers Appl.* **2007**, *1*, 1.
- Bannes, C. P.; Sell, S. A.; Knapp, D. C.; Walpoth, B. H.; Brand, D. D.; Bowlin, G. L. *Int. J. Electrospun Nanofibers Appl.* **2007**, *1*, 73.
- Welle, A.; Kroeger, M.; Doering, M.; Niederer, K.; Pindel, E.; Chronakis, L. S. *Biomaterials* **2007**, *28*, 2211.

8. Gupta, A.; Saquing, C. D.; Afshari, M.; Tonelli, A. E.; Khan, S. A.; Kotek, R. *Macromolecules* **2009**, *42*, 709.
9. Deitzel, J. M.; Kleinmeyer, J.; Harris, D.; Beck Tan, N. C. *Polymer* **2001**, *42*, 261.
10. Nitanan, T.; Opanasopit, P.; Akkaramongkolporn, P.; Rojanarata, T.; Ngawhirunpat, T.; Supaphol, P. *Korean J. Chem. Eng.* **2012**, *29*, 173.
11. You, Y.; Lee, S. J.; Min, B.-M.; Park, W.-H. *J. Appl. Polym. Sci.* **2006**, *99*, 1214.
12. Wannatong, L.; Sirivat, A.; Supaphol, P. *Polym. Int.* **2004**, *53*, 1851.
13. Lee, K. H.; Kim, H. Y.; Bang, H. J.; Jung, Y. H.; Lee, S. G. *Polymer* **2003**, *44*, 4029.
14. Entov, V. M.; Shmaryan, L. E. *Fluid Dyn.* **1997**, *32*, 696.
15. Fong, H.; Chun, I.; Renker, D. H. *Polymer* **1999**, *40*, 4585.
16. Eda, G.; Shivkumar, S. *J. Mater. Sci.* **2006**, *41*, 5704.
17. Andraday, A. L. *Science and Technology of Polymer Nanofibers*; Wiley: Hoboken, NJ, **2008**; Chapter 3, p 71.
18. Qin, X. H.; Yang, E. L.; Li, N.; Wang, S. Y. *J. Appl. Polym. Sci.* **2007**, *103*, 3865.
19. Lin, T.; Wang, H. X.; Wang, H. M.; Wang, X. G. *Nanotechnology* **2004**, *15*, 1375.
20. Chen, Y. Z.; Peng, P.; Guo, Z. X.; Yu, J.; Zhan, M. S. *J. Appl. Polym. Sci.* **2010**, *115*, 3687.
21. Choi, J. S.; Lee, S. W.; Jeong, L.; Ba, S. H.; Min, B. C.; Youk, J. H.; Park, W. H. *Int. J. Biol. Macromol.* **2004**, *34*, 249.
22. Cheng, W.; Yu, Q.; Qiu, Z.; Yan, Y. *J. Appl. Polym. Sci.* **2013**, *130*, 2359.
23. Bhardwaj, N.; Kundu, S. C. *Biotechnol. Adv.* **2010**, *28*, 325.
24. Patra, S. N.; Easteal, A. J.; Bhattacharyya, D. *J. Mater. Sci.* **2008**, *44*, 647.
25. Yuan, X. Y.; Zhang, Y. Y.; Dong, C. H.; Sheng, J. *Polym. Int.* **2004**, *53*, 1704.
26. Zhang, C.; Yuan, X.; Wu, L.; Han, Y.; Sheng, J. *Eur. Polym. J.* **2005**, *41*, 423.
27. Ki, C. S.; Baek, D. H.; Gang, K. D.; Lee, K. H.; Um, I. C.; Park, Y. H. *Polymer* **2005**, *46*, 5094.
28. Costa-Pinto, A. R.; Martins, A. M.; Castelhana-Carlos, M. J.; Correló, V. M.; Sol, P. C.; Filho, A. L.; Battacharya, M.; Reis, R. L.; Neves, N. M. *J. Bioact. Compat. Polym.* **2014**, *29*, 137.
29. Xu, J.; Guo, B. H. *Biotechnol. J.* **2010**, *5*, 1149.
30. Rudnik, E. *Compostable Polymer Materials*; Elsevier: Oxford, United Kingdom, **2008**; Chapter 3, p 52.
31. Sutthiphong, S.; Pavasant, P.; Supaphol, P. *Polymer* **2009**, *50*, 1548.
32. Tian, L.; Wang, P.; Zhao, Z.; Ji, J. *Appl. Biochem. Biotechnol.* **2013**, *171*, 1890.
33. Jeonga, E. H.; Imb, S. S.; Youk, J. H. *Polymer* **2005**, *46*, 0538.
34. Tserki, V.; Filippou, I.; Panayiotou, C. *Proc. IMechE Part N: J. Nanoeng. Nanosys.* **2006**, *220*, 71.
35. Eastman. Solvent Selector Chart. Available at http://www.eastman.com/Literature_Center/M/M167.pdf (accessed October 20, 2014).
36. Mozga, W. Physical properties of liquids. Available at <http://www.trimen.pl/witek/ciecze/liquids.html> (accessed January 12, 2015).
37. Tanaka, T.; Takahashi, M.; Kawaguchi, S.; Hashimoto, T.; Saitoh, H.; Kouya, T.; Taniguchi, M.; Douglas, R. S. L. *Desalin. Water Treat.* **2010**, *17*, 176.
38. Moghe, A. K.; Hufenus, R.; Hudson, S. M.; Gupta, B. S. *Polymer* **2009**, *50*, 3311.
39. Seo, J. M.; Arumugam, G. K.; Khan, S.; Heiden, S. P. *Macromol. Mater. Eng.* **2009**, *294*, 35.
40. Manee-in, J.; Nithitanakul, M.; Supaphol, P. *Iran. Polym. J.* **2006**, *15*, 341.
41. Casasola, R.; Thomas, N. L.; Trybala, A.; Georgiadou, S. *Polymer* **2014**, *55*, 4728.
42. Tungprapan, T.; Puangparn, T.; Weerasombut, M.; Jangchud, I.; Fakum, P.; Semongkhon, S.; Meechaisue, C.; Supaphol, P. *Cellulose* **2007**, *14*, 563.
43. Mit-uppatham, C.; Nithitanakul, M.; Supaphol, P. *Macromol. Chem. Phys.* **2004**, *205*, 2327.
44. Supaphol, P.; Mit-uppatham, C.; Nithitanakul, M. *J. Polym. Sci. Polym. Phys.* **2005**, *43*, 3699.
45. Veleirinh, B.; Rei, M. F.; Lopes-da-Silva, J. A. *J. Polym. Sci., Part B: Polym. Phys.* **2008**, *46*, 460.